

https://doi.org/ 10.35895/jpsi.1.2.136-144.2025

# The Effect of Quartz Sand on Structural and Optical Properties of Dy<sup>3+</sup> Doped P<sub>2</sub>O<sub>5</sub>-CaO-BaO-Gd<sub>2</sub>O<sub>3</sub> Glasses

Jonny H. Panggabean<sup>1</sup>, Novita Madalena Br Sembiring<sup>1</sup>, Elyzabeth Simanullang<sup>1</sup>, Juniastel Rajagukguk<sup>1\*</sup>, C.S. Sarumaha<sup>2</sup>, J. Kaewkhao<sup>2,3</sup>

<sup>1</sup>Department of Physics, Faculty of Mathematics and Natural Sciences, Universitas Negeri Medan,
Deli Serdang, 20371, Indonesia

<sup>2</sup>Faculty of Science and Technology, Muban Chombueng Rajabhat University, Ratchaburi, 70150, Thailand

<sup>3</sup>Center of Excellence in Glass Technology and Materials Science (CEGM), Nakhon Pathom Rajabhat University,
Nakhon Pathom, 73000, Thailand

(Received September 25, 2025; revised October 20, 2025; accepted October 28, 2025; published online October 31, 2025)

This study investigates the influence of quartz sand incorporation on the structural and optical properties of Dy³+ doped P₂O₅-CaO-BaO-Gd₂O₃ phosphate glasses. The glass samples were synthesized using the conventional melt-quenching technique, with varying concentrations of quartz sand as a partial substitution of P₂O₅. Structural characterization was carried out using X-ray diffraction (XRD) and Fourier transform infrared (FTIR) spectroscopy, which confirmed the formation of an amorphous glass network and the presence of phosphate, silicate, and modifier-related vibrational bands. The optical absorption spectra, recorded via UV−Vis spectroscopy, revealed characteristic f−f transitions of Dy³+ ions, indicating their successful incorporation into the glass matrix. The intensity ratio of yellow to blue emission was found to be influenced by the quartz sand content, suggesting a significant role of SiO₂ in modifying the local environment around Dy³+ ions. These results highlight the potential of quartz-sand-modified phosphate glasses as promising candidates for photonic and luminescent device applications.

**Keywords:** Dy<sup>3+</sup> doping, phosphate glass, photoluminescence, Quartz sand, structural properties



This is an open access article under the <u>CC BY-NC</u> license. Copyright © 2025 by Author. Published by Physical Society of Indonesia

### 1. INTRODUCTION

In recent years, research on phosphate glass-based materials has grown rapidly due to their potential in various technological applications, especially in the fields of optics and electronics. Phosphate glass has unique optical and thermal properties, so it is widely used in the manufacture of lasers, medical imaging devices, and sensors. One way to improve the optical and physical properties of phosphate glass is by doping it with rare earth ions, which can improve its luminescence performance (Milanese, 2017; Amjad et al., 2020). Quartz sand is one of the materials widely used in glass manufacturing because of its transparent properties across a wide spectrum, and it has good thermal conductivity. The presence of quartz sand in the phosphate glass medium can affect its physical structure, such as density, viscosity, and other mechanical properties (Sharma, 2018; Panggabean et al., 2024). Glass is an amorphous solid material produced from the rapid cooling of mineral melts, especially silica (SiO2).

Glass has four types, namely silicate glass, phosphate glass, borate glass, and teleruite glass. The selection of phosphate glass as the main medium is based on its advantages compared to silicate glass or borate glass. Phosphate glass has the ability to dissolve high amounts of rare earth ions, which allows for increased luminescence emission intensity (Norkus et al., 2021). However, the weakness of phosphate glass is its relatively low resistance to water and aggressive environments. Therefore, the addition of quartz sand is expected to increase the resistance of phosphate glass to chemical degradation

\*Contact Author: juniastel@unimed.ac.id

ISSN: 2685-3841 (Online)

(Panggabean et al., 2024). The addition of Dy3+ ions to the phosphate glass medium aims to increase the efficiency of light emission in a certain spectral range, so that it can be used for applications such as optical displays and active materials in lasers (Mahamuda et al., 2021). Dy3+ ions are known to have excellent luminescence characteristics, so they can be utilized in various optical applications such as lasers, radiation dosimeters, and fluorescent sensors (Huerta et al., 2020). Variations in the composition and ratio of phosphate to SiO2 can lead to changes in optical parameters, such as the refractive index and absorption coefficient, which directly impact material performance in optoelectronic applications (Amarnath Reddy et al., 2011).

This research is expected to provide new insights into strategies for optimizing glass material composition for various functional applications. These findings can also serve as a reference for further research in the field of optical and electronic materials, as well as contribute to the development of rare earth-based technologies (Linganna et al., 2014). This research will utilize the melt quenching method, which is widely favored due to its simplicity and ability to produce highly homogeneous glass structures.

## 2. METHOD

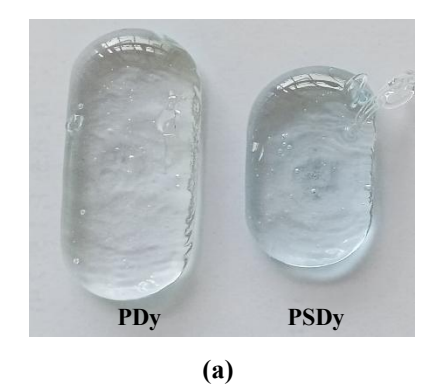
The procedure for making a glass medium based on Huta Ginjang quartz sand involves preparing quartz sand taken from Huta Ginjang. Afterward, the quartz sand is cleaned by separating it from impurities, washing it, and drying it in sunlight. A ball mill is a method of refining the quartz sand into powder for 4 hours. The glass materials used are prepared in mol% units as follows: First sample (PDy) 74.5P<sub>2</sub>O<sub>5</sub> – 15CaO – 5BaO – 5Gd<sub>2</sub>O<sub>3</sub> – 0.5Dy<sub>2</sub>O<sub>3</sub>, Second sample (PSDy) 15QS – 59.5P<sub>2</sub>O<sub>5</sub> – 15CaO – 5BaO – 5Gd<sub>2</sub>O<sub>3</sub> – 0.5Dy<sub>2</sub>O<sub>3</sub>. Each material is weighed using a digital scale according to the predetermined mass of each material. Mixing the materials homogeneously with a spatula, stirred manually in an alumina crucible. Insert the alumina container into a jar containing silica gel to reduce the water vapor in the material, and let it stand for 24 hours in a vacuum chamber. The evenly mixed material is put into a furnace at a temperature of 1200°C for approximately 3 hours for the melting process of the glass material, then all the materials melt and reach a good state, and produce a glass material that is not cracked, and then poured into a rectangular stainless steel mold. The printed sample is then carried out in an annealing process with a heating time of 3 hours at a temperature of 500°C and cooled slowly to room temperature. The glass sample is cut to a size of 1cm x 0.3 cm x 1.5 cm. The refined sample will be characterized using FTIR, XRD, and processed and analyzed data.

### 3. RESULT AND DISCUSSION

# 3.1 Glass Sample

ISSN: 2685-3841 (Online)

Samples that have been successfully prepared with a combination of PDy and PSDy are shown in Figure 1.



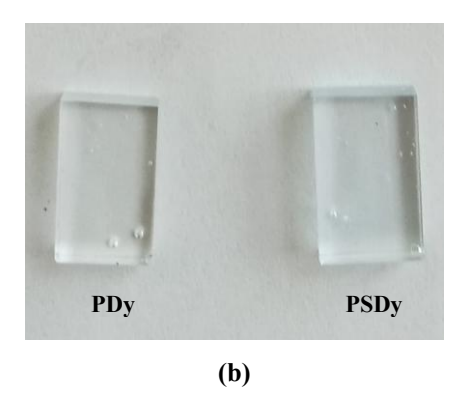


**Figure 1**. Sample display of Dysprosium-doped Gadolinium Phosphate with Dy<sup>3+</sup> (a) before cutting and polishing, (b) after being cut and polished

Figure 1 (a) (oval shape) shows a phosphate glass sample in its initial melted state, which is common during the glass melting process. Figure 1 (b) shows a phosphate glass sample that has been cut and polished into a small glass plate. From a physical structural perspective, the glass sample appears clear and transparent, indicating that the material is amorphous with a uniform phase distribution. This transparency is important in optical applications, such as photonic materials, laser media, or luminescent devices.

# 3.2 Absorption Spectrum

The spectrum of the glass shows two transition points from the ultraviolet to the infrared spectrum (UV-Vis-NIR). These peaks are found at wavelengths between 300 and 2500 nm, as shown in Figure 2.

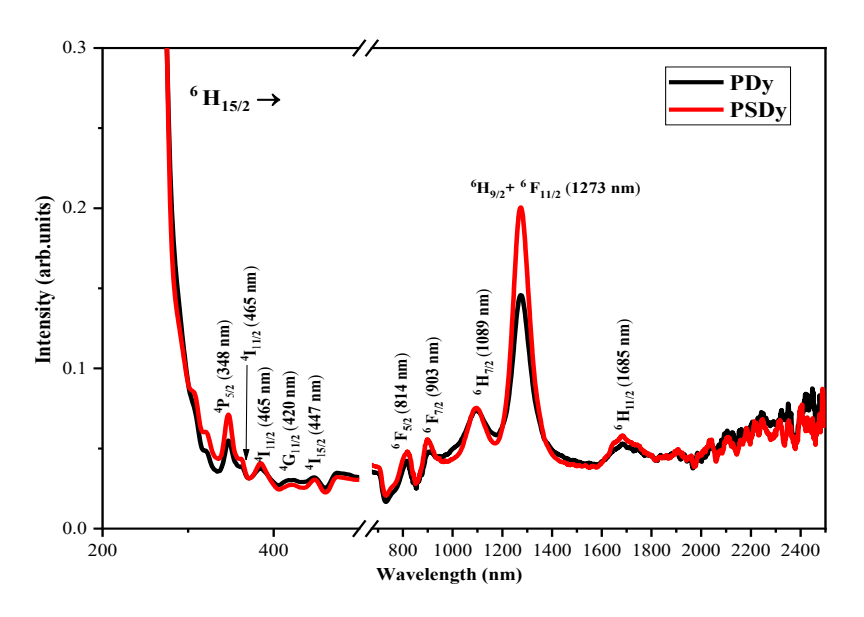


Figure 2. Absorption spectrum graph of glass doped with Dy<sup>3+</sup> ions

The localized f-f transition of the 4f electron in the Dy³+ ion undergoes a transition between multiplets, after the spectrum shows sharp lines (multiplets) originating from transitions between states separated by spin-orbit and crystal field. Selection rules and weak intensity: the f-f transition is parity-forbidden in the symmetry center approximation, so its intensity is relatively weak; the real intensity arises through mixing with orbitals of different parity (odd-parity vibronic coupling or host-induced mixing). The Judd-Ofelt theory is often used to quantify the intensity of the f-f transition in lanthanides. Host effect (glass vs. crystal): In glass, local disorder broadens the spectral lines (broadening), eliminating some of the subtle features seen in ordered crystals.

Additionally, network modifiers (e.g., CaO, BaO, Gd<sub>2</sub>O<sub>3</sub>, or SiO<sub>2</sub> from quartz sand) alter the local field around Dy<sup>3+</sup>, thereby shifting the peak positions and changing the intensity ratio of the emission lines.  $^6H_{15/2}$  is the initial emission of Dy<sup>3+</sup> 453 nm, 475 nm, 447 nm transition  $^4I_{15/2} \rightarrow ^6H_{15/2}$ ,  $^4F_{9/2}$ , transitions in the blue band 814 nm transition  $^6F_{9/2}$  is a near infrared emission 908 nm, 1098 nm transition  $^6H_{13/2}$ ,  $^6H_{11/2}$  is a transition to a lower energy level 1273 nm transition  $^6H_{13/2} + ^6F_{11/2}$  is the main emission peak in the NIR region 1685 nm, 1985 nm  $^6H_{9/2}$  is the emission in the long NIR region of the intensity in almost the entire spectrum compared to PDy (black). The main peak around 1273 nm is very dominant, indicating the high emission efficiency of the Dy<sup>3+</sup> transition in PSDy material (Biradar et al., 2024; Thakur, 2020)

## 3.3 Photoluminescence (PL) Spectra

ISSN: 2685-3841 (Online)

A number of sharp peaks indicating specific transitions of rare earth metal ions, especially the transitions from Gd³+ (in blue color), 275 nm ( $^8S_{7/2} \rightarrow ^6I_{7/2}$ ) 245, 253, 263 nm Transitions of  $^8S_{7/2} \rightarrow ^6P_J$  or  $^6D_J$  are shown in Figure 3.

ISSN: 2685-3841 (Online)

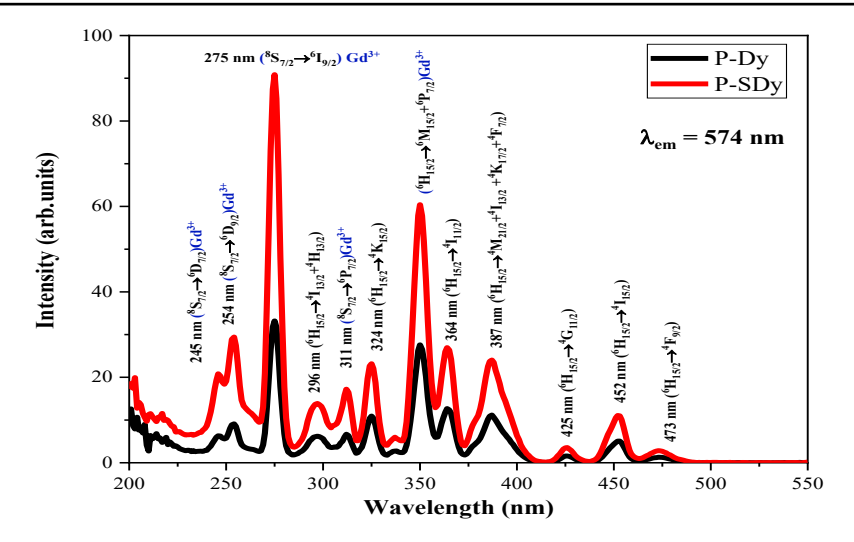


**Figure 3.** Excitation spectrum graph with  $\lambda_{em}$ = 574 nm

This Gd<sup>3+</sup> transition functions as a sensitizer-absorbing UV energy and transferring it to Dy<sup>3+</sup>. The transition from Dy<sup>3+</sup> 290-480 nm, transitions from the ground state  $^6H_{15/2}$  to various excited states, such as:  $^6P_{7/2}$ ,  $^4I_{13/2}$ ,  $^6F_{7/2}$ , and others. The P-SDy sample shows higher excitation intensity at almost all wavelengths than P-Dy. This indicates that the modification/addition of Gd<sup>3+</sup> to the PSDy system provides better energy transfer efficiency, enhancing the excitation of Dy<sup>3+</sup>, resulting in stronger emission at 574 nm (Khrongchaiyaphum et al., 2022). The sharp emission peak indicates a weak intra-4f transition of Dy<sup>3+</sup> under the influence of the crystal field, but the relative intensity of the peak can be influenced by the host glass composition. The increased luminescence intensity in P-SDy indicates that modification of the glass composition can increase the local symmetry and reduce quenching, thus making the Dy<sup>3+</sup> radiative transition stronger (Shen et al., 2020; Lakshminarayana et al., 2017). The emission spectrum displays four total peaks, namely  $^4P_{9/2} \rightarrow ^6H_{15/2}$  (482 nm),  $^4P_{9/2} \rightarrow ^6H_{13/2}$  (573 nm),  $^4P_{9/2} \rightarrow ^6H_{11/2}$  (663 nm), and  $^4P_{9/2} \rightarrow ^6H_{9/2}$  (753 nm) as shown in Figure 4.

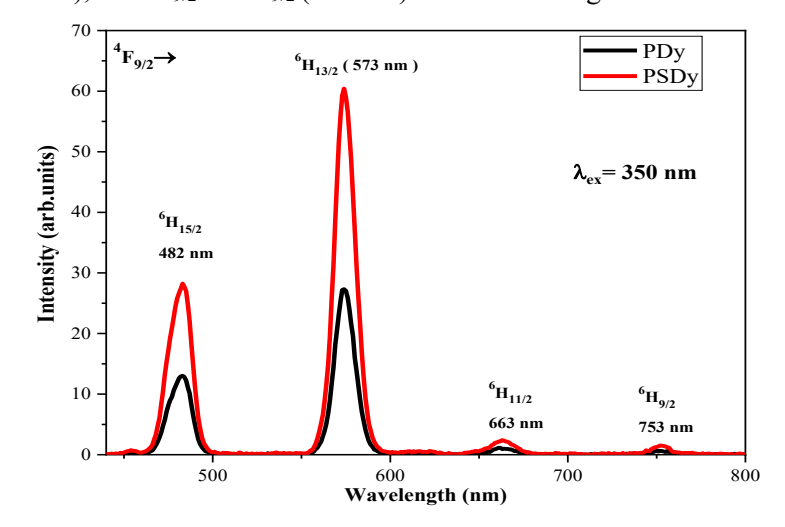


Figure 4. Emission spectrum with 350 nm excitation wavelength of Dy<sup>3+</sup>glass

This spectrum phenomenon indicates that the glass system has the potential to be applied as a photonic material, especially in the development of yellow phosphors and white light sources based on Dy<sup>3+</sup>, because the blue–yellow emission ratio can be adjusted through the host composition (Nath & Biswas, 2023; Zhuk et al., 2023). Photoluminescence (PL) spectra of Dy<sup>3+</sup> glasses with an excitation wavelength of 350 nm. PSDy shows much higher emission intensity, especially at a wavelength of 275 nm, as shown in Figure 5. This indicates better energy transfer efficiency, possibly due to additional doping (Kumar et al., 2023)

ISSN: 2685-3841 (Online)

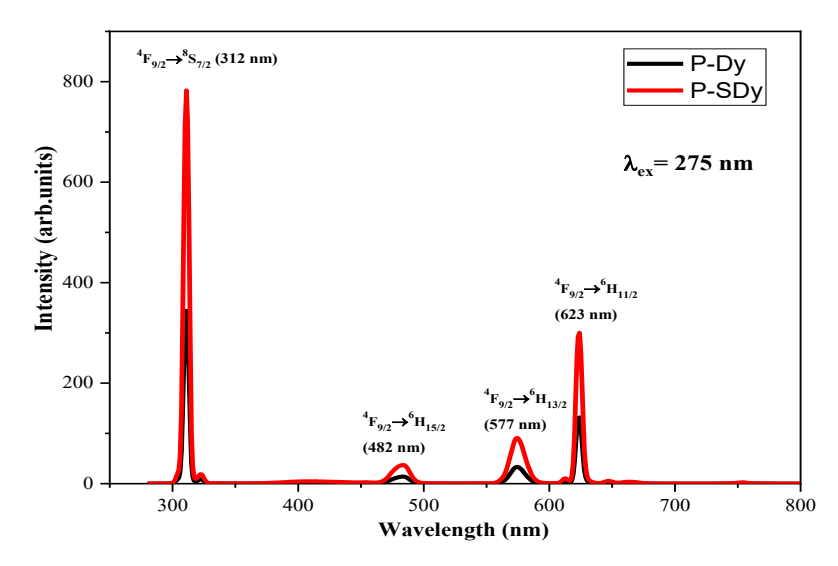


Figure 5. Emission spectrum under Dy<sup>3+</sup>

Emission images under Dy³+, Wavelength (nm) 312 nm  $^6P_{7/2} \rightarrow ^8S_{7/2}$  Gd³+ (Sharp emission from Gd³+ ions), 482 nm  $^4F_{9/2} \rightarrow ^6H_{15/2}$  Dy³+, 577 nm  $^4F_{9/2} \rightarrow ^6H_{15/2}$  Dy³+, 623 nm  $^4F_{9/2} \rightarrow ^6H_{15/2}$  Dy³+ (weak red emission). The 312 nm band (Gd³+) shows very high intensity, indicating that Gd³+ ions play an important role in the energy transfer process to Dy³+. The intensity increases at all Dy³+ emission peaks. Possible co-doping effect of Gd³+ or increased crystallinity, which favors energy transfer from Gd³+  $\rightarrow$  Dy³+ (Li et al., 2020; Gupta et al., 2024; Ullah et al., 2022)

The emission transition from  $Dy^{3+}$  produces a visible light spectrum, which is important for optoelectronic applications such as phosphor LEDs.  $Gd^{3+}$  ions have high energy levels and can absorb excitation energy at 275 nm (UV). This energy is then transferred to  $Dy^{3+}$ , which emits in the visible (blue-yellow-red) region. This process is very efficient in PSDy (Neupane et al., 2022). Important spectral parameters such as emission peak wavelength ( $\lambda_p$ ), effective bandwidth ( $\Delta\lambda$ eff), emission cross section ( $\sigma_e$ ), emission branching ratio ( $\beta$ ), and radiation rate (AR). The transitions  ${}^4F_{9/2} \rightarrow {}^6H_{15/2}$  and  ${}^6H_{13/2}$  appear at about 483 nm and 573 nm, respectively, which are the two dominant peaks of typical emission of  $Dy^{3+}$  ions, as shown in Table 1.

**Table 1.** The peak emission wavelength  $(\lambda_p)$ , effective *bandwidth*  $(\Delta \lambda_{eff})$ , emission cross section  $(\sigma_e(\lambda_p) \times 10^{(-22)})$ , branching ratio  $(\beta_R)$ , and radioactive transition probability (AR) are the radioactive characteristics of Sm glass.

Glass	Transition	$\lambda_{\mathrm{p}}$	$\Delta \lambda_{ m eff}$	$\sigma_{e}(\lambda_{p})$	βexp	βcal	AR	$ au_{ m R}$	
	$^4\mathrm{F}_{9/2}$ $\longrightarrow$	(nm)	(nm)	(cm <sup>2</sup> )	(%)	(%)	$(s^{-1})$	J-O (ms)	Exp (ms)
Pdy	$^{6}\mathrm{H}_{15/2}$	483	23.32	0.206	0.3494	0.0776	15.82	4903	0.652
	$^{6}\mathrm{H}_{13/2}$	573	19.98	2.45	0.6219	0.4001	81.59		
	$^{6}\mathrm{H}_{11/2}$	663	15.62	1.25	0.0210	0.089	18.16		
	$^{6}\mathrm{H}_{9/2}$	753	13.33	0.614	0.0077	0.0234	4.770		
PSDy	$^{6}\mathrm{H}_{15/2}$	483	23.42	0.236	0.2811	0.1071	18.20	5885	0.662
	$^{6}\mathrm{H}_{13/2}$	573	26.42	1.17	0.6952	0.303	51.48		
	$^{6}\mathrm{H}_{11/2}$	663	16.44	0.911	0.0162	0.0819	13.91		
	$^{6}\mathrm{H}_{9/2}$	753	11.33	0.661	0.0075	0.0246	4.180		

Maximum intensity occurs at 573 nm, which is indicated by the largest emission cross section  $(\sigma_e)$  value and the highest emission branch ratio  $(\beta_{exp})$ . The highest  $\sigma_e$  value is found at the transition to  ${}^6H_{13/2}$  in PDy glass  $(2.45 \times 10^{-20} \text{ cm}^2)$ , indicating strong emission efficiency in the yellow region (Gai et al., 2024). This is also evident from the large AR value at this transition. In both glasses, the transition to  ${}^6H_{13/2}$  dominates, with  $\beta_{exp}$  values reaching 62.19% (PDy) and 69.52% (PSDy). This indicates that the

majority of the emission occurs in the yellow region, which is important for white lighting applications. The transition to  ${}^6\mathrm{H}_{15/2}$  (blue) remains significant, so the blue-yellow comparison can be used to evaluate the color balance (Thanyaphirak et al., 2024; Lakshminarayana et al., 2020)

### 3.4 Lifetime

Figure 6 (a) The longer emission lifetime of PGdO (3.520 ms) indicates that the oxide structure is able to form strong bonds that stabilize the excited state and slow down non-radiative relaxation. In contrast, the shorter lifetime of PGdF (2.488 ms) indicates that, despite having a low phonon energy, the possible presence of defects or structural irregularities accelerates the relaxation process. Thus, higher photoluminescence emission efficiency is exhibited by PGdO, making it more suitable for applications such as dosimeters, optical sensors, and bioimaging phosphors that require delayed emission. Meanwhile, PGdF is more suitable for applications that require fast response and high thermal stability (Deshmukh et al., 2024).

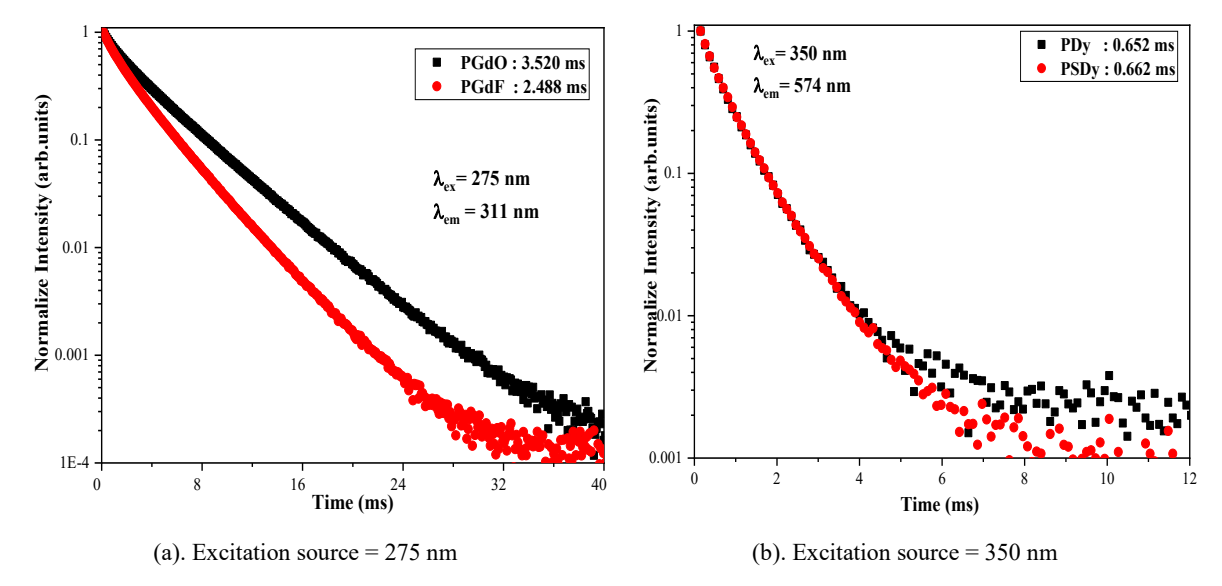


**Figure 6.** Lifetime of glasses (a) with excitation wavelength of 275 nm and emission wavelength of 311 nm, or (b) with excitation wavelength of 350 nm and emission wavelength of 574 nm

Figure 6 (b) shows the exponential curve of luminescence decay of Dy<sup>3+</sup> ions at 574 nm wavelength after excitation at 350 nm. Black for PDy with a lifetime of 0.652 ms, red for PSDy with a lifetime of 0.662 ms. Both samples show exponential decay, typical of the electronic transition of lanthanide ions such as Dy<sup>3+</sup>. The PSDy sample has a slightly longer lifetime (0.662 ms) than PDy (0.652 ms), suggesting that the modification performed (addition of quartz sand) provides a slight improvement in the stability of the excited state of Dy<sup>3+</sup> ions (Jiménez et al., 2024)

### 3.5 Judd-Ofelt parameter and Radiative properties

The experimental oscillator strength (fexp), calculated for each transition present in the absorption spectrum, and the calculated oscillator strength (fcal) values are obtained using the Judd-Ofelt software and theory. The experimental oscillator strength indicates the quantum probability of a transition and the intensity of each absorption band. This shows that increasing the oscillator strength can increase the intensity of the absorption band, which is very important for broad absorption spectra (Đačanin Far et al., 2018). Table 1 illustrates the calculation results of the oscillator strength values. The fexp and fcal values have been prepared along with the rms values. The rms values show a good agreement between the fexp and fcal values, which indicates the applicability of the J-O theory. Intensity parameters in Table 2.

The table shows the spectral transitions from the ground state  ${}^{6}H_{5/2}$  to the excited state of Dy<sup>3+</sup> ions in PDy and PSDy glass matrices. The absorption wavelength ( $\lambda_{abs}$ ), transition energy ( $E_{exp}$ ), as well as oscillator strength values ( $f_{exp}$  and  $f_{cal}$ ) were evaluated both experimentally and theoretically. In

general, the difference between  $f_{exp}$  and  $f_{cal}$  values shows a match that varies depending on the transition (Mika et al., 2013). For example, the transition  ${}^{6}H_{5/2} \rightarrow {}^{6}F_{11/2}$  shows excellent agreement between experimental and calculated results for both PDy ( $f_{exp} = 0.542$ ;  $f_{cal} = 0.540$ ) and PSDy ( $f_{exp} = 0.766$ ;  $f_{cal} = 0.763$ ). In contrast, at transitions such as  ${}^{6}H_{5/2} \rightarrow {}^{4}F_{9/2}$ , noticeable differences are observed, especially in the PDy sample, which may be caused by local structure mismatches or other nonradiative factors. The  $\delta_{rms}$  (root mean square deviation) value is used to evaluate the overall agreement between experimental and calculated values. It is found that PSDy has a lower  $\delta_{rms}$  value (0.122) than PDy (0.298), which indicates that the theoretical model is more suitable for the PSDy system (Đačanin Far et al., 2018).

**Table 2.** Experimental oscillator strength  $(f_{exp})$  and calculated oscillator strength  $(f_{cal})$  on Dy<sup>3+</sup> glass

Transition			Po	Pdy		Dy
<sup>6</sup> H <sub>5/2</sub> →	$\lambda_{abs}(nm)$	$E_{exp}$ (cm <sup>-1</sup> )	$f_{ m exp}$	$f_{ m cal}$	$f_{ m exp}$	$f_{ m cal}$
<sup>6</sup> P <sub>7/2</sub>	349	28653.3	0.138	0.068	0.149	0.060
$^{4}K_{17/2}$	387	25839.79	0.038	0.098	0.063	0.102
$^{4}I_{15/2}$	450	22222.22	0.008	0.057	0.068	0.061
$^{4}F_{9/2}$	479	20876.83	0.597	0.023	0.027	0.176
$^{6}F_{5/2}$	821	12180.27	0.142	0.144	0.207	0.127
$^{6}F_{7/2}$	901	11098.78	0.277	0.305	0.205	0.223
$^{6}\mathrm{H}_{7/2}$	1098	9107.47	0.689	0.012	0.351	0.010
$^{6}F_{11/2}$	1280	7812.5	0.542	0.540	0.766	0.763
$^{6}\mathrm{H}_{11/2}$	1686	5931.2	0.144	0.160	0.146	0.171
$\delta_{ m rms}$			0.298		0.122	

**Table 3.** J-O parameters (x 10<sup>-20</sup>) of glass Phosphate doped Dy<sup>3+</sup> ion

Glass	$\Omega_2$	$\Omega_4$	$\Omega_6$	$\chi(\Omega_4/\Omega_6)$	Trend	Source
Pdy	0.499	0.234	0.365	0.641	$\Omega_2 > \Omega_6 > \Omega_4$	Sample
PSDy GS35 DyCaAS	1.144 10.73 7.36	0.118 0.11 0.18	0.323 0.13 1.49	0.365 0.846 0.120	$\begin{split} &\Omega_2 > \Omega_6 > \Omega_4 \\ &\Omega_2 > \Omega_6 > \Omega_4 \\ &\Omega_2 > \Omega_6 > \Omega_4 \end{split}$	Sample Li et al. (2020) Zekri et al. (2019)

Judd-Ofelt parameters ( $\Omega_{\lambda}$ , with  $\lambda$ =2,4,6) are used to evaluate the local environment and strength of dipole electric transitions in lanthanide ions, including Dy³+. These values are very useful for understanding the local symmetry and covalent bonding of metal ions in glass matrices. Higher values of  $\Omega_2$  indicate a greater degree of covalency and asymmetry of the local environment around Dy³+ ions. (Kumar et al., 2023). In the PSDy sample, the  $\Omega_2$  reaches 1.144, much higher than that of PDy (0.499), indicating that additional doping or matrix modification in PSDy increases the local disorder around Dy³+ ions. The trends of Judd-Ofelt parameters for both samples show the same pattern, i.e.,  $\Omega_2 > \Omega_6 > \Omega_4$ , which indicates the dominance of dipole electric transitions amplified by local unsymmetrical neighborhoods and indicates the characteristics of amorphous structures. The smaller  $\chi$  = ratio value of  $\Omega_4/\Omega_6$  in PSDy (0.365) compared to PDy (0.641) indicates the possibility of enhanced nonradiative relaxation or the influence of a more homogeneous environment in inhibiting  $\Omega$ 4-related transitions.

#### 4. CONCLUSION

This study shows that the addition of quartz sand as a partial substituent for P<sub>2</sub>O<sub>5</sub> in the P<sub>2</sub>O<sub>5</sub>–CaO–BaO–Gd<sub>2</sub>O<sub>3</sub> glass system doped with Dy<sup>3+</sup> ions significantly affects the structural and optical properties of the material. The results of XRD and FTIR analyses confirm that all samples retain their amorphous nature, with the formation of vibration bands indicating the presence of phosphate and silicate groups in the glass network. The UV–Vis absorption spectra display typical f–f transitions of

Dy<sup>3+</sup> ions, indicating successful integration of the dopant into the glass matrix, with the ratio of yellow to blue intensity affected by the quartz sand content. This indicates that the presence of SiO<sub>2</sub> modifies the local environment of Dy<sup>3+</sup> through changes in the symmetry and covalent bonding, which in turn affects the optical characteristics of the material. Overall, the results of this study confirm that modification using quartz sand not only maintains the structural properties of phosphate glasses but also improves the controllability of the blue–yellow emission ratio of Dy<sup>3+</sup>. Thus, quartz sand-modified phosphate glass has the potential to be developed as a candidate material for photonic applications, including yellow-emitting phosphors and white-light-based luminescent devices.

#### ACKNOWLEDGMENTS

The authors would like to thank Universitas Negeri Medan for supporting this project with contract no. 037/UN33.8/PPKM/PD/2025. The authors also thank the Thailand Institute for Science Research and Innovation and Nakhon Pathom Rajabhat University for their assistance with this research.

#### REFERENCES

ISSN: 2685-3841 (Online)

- Amarnath Reddy, A., Chandra Sekhar, M., Pradeesh, K., Surendra Babu, S., & Vijaya Prakash, G. (2011). Optical properties of Dy3+-doped sodium–aluminum–phosphate glasses. *Journal of Materials Science*, 46(7), 2018–2023. https://doi.org/10.1007/s10853-010-4851-3
- Amjad, R. J., Sattar, A., & Dousti, M. R. (2020). Upconversion and 1.53 μm near-infrared luminescence study of the Er3+-Yb3+ co-doped novel phosphate glasses. *Optik*, 200, 163426. https://doi.org/10.1016/j.ijleo.2019.163426
- Biradar, S., Dinkar, A., & Devidas, G. B. (2024). Optical Modifications in Eu2O3 Doped Borate Glasses: Impact on Bandgap, Metallicity, and Photonic Properties. *Nexus of Future Materials*, *None*(None). https://doi.org/10.70128/588347
- Đačanin Far, Lj., Lukić-Petrović, S. R., Đorđević, V., Vuković, K., Glais, E., Viana, B., & Dramićanin, M. D. (2018). Luminescence temperature sensing in the visible and NIR spectral range using Dy3+ and Nd3+ doped YNbO4. Sensors and Actuators A: Physical, 270, 89–96. https://doi.org/10.1016/j.sna.2017.12.044
- Deshmukh, R. K., Swamy, N. K., Verma, O. P., & Dubey, V. (2024). Luminescence Materials Used for Dosimeter and Applicationts; a Comprehensive Review. In *Futuristic Trends in Physical Sciences Volume 3 Book 1* (pp. 39–84). Iterative International Publishers, Selfypage Developers Pvt Ltd. https://doi.org/10.58532/V3BKPS1CH4
- Gai, S., Gao, P., Chen, K., Tang, C., Zhao, Y., Wei, J., Zhang, Y., Molokeev, M. S., Xia, M., & Zhou, Z. (2024). Superior Quantum Efficiency Blue-Emitting Phosphors with High Thermal Stability toward Multipurpose LED Applications. *Advanced Optical Materials*, 12(14), 202302870. https://doi.org/10.1002/adom.202302870
- Gupta, S. K., Jafar, M., Thekke Parayil, R., Bahadur, J., & Sudarshan, K. (2024). White light emitting nanocrystalline Y1–Gd PO4:Dy3+ and improved PLQY on Gd3+ co-doping. *Inorganic Chemistry Communications*, 159, 111908. https://doi.org/10.1016/j.inoche.2023.111908
- Huerta, E. F., Meza-Rocha, A. N., Lozada-Morales, R., Speghini, A., Bordignon, S., & Caldiño, U. (2020). White, yellow and reddish-orange light generation in lithium-aluminum-zinc phosphate glasses co-doped with Dy3+/Tb3+ and tri-doped with Dy3+/Tb3+/Eu3+. *Journal of Luminescence*, 219, 116882. https://doi.org/10.1016/j.jlumin.2019.116882
- Jiménez, J. A., Hedge, V., Viswanath, C. S. D., & Amesimenu, R. (2024). Insights into the Structural, Thermal/Dilatometric, and Optical Properties of Dy <sup>3+</sup> -Doped Phosphate Glasses for Lighting Applications. *ACS Physical Chemistry Au*, 4(6), 720–735. https://doi.org/10.1021/acsphyschemau.4c00066
- Khrongchaiyaphum, F., Wantana, N., Sarumaha, C. S., Kaewnuam, E., Kothan, S., Chanthima, N., & Kaewkhao, J. (2022). Optical, luminescence, and energy transfer studies of Gd3+/Dy3+ doped potassium gadolinium borophosphate glasses. *Radiation Physics and Chemistry*, 201, 110442. https://doi.org/10.1016/j.radphyschem.2022.110442
- Kumar, P., Singh, S., Gupta, I., Nehra, K., Kumar, V., & Singh, D. (2023). Structural and luminescent behaviour of Dy(III) activated Gd3Al5O12 nanophosphors for white-LEDs applications. *Materials Chemistry and Physics*, 295, 127035. https://doi.org/10.1016/j.matchemphys.2022.127035

ISSN: 2685-3841 (Online)

- Lakshminarayana, G., Kaky, K. M., Baki, S. O., Lira, A., Caldiño, U., Kityk, I. V., & Mahdi, M. A. (2017). Optical absorption, luminescence, and energy transfer processes studies for Dy3+/Tb3+-codoped borate glasses for solid-state lighting applications. *Optical Materials*, 72, 380–391. https://doi.org/10.1016/j.optmat.2017.06.030
- Lakshminarayana, G., Wagh, A., Lira, A., Kityk, I. V., Lee, D.-E., Yoon, J., & Park, T. (2020). Dy3+: B2O3–Al2O3–ZnO–Bi2O3–BaO–M2O (M=Li; Na; and K) glasses: Judd–Ofelt analysis and photoluminescence investigation for WLED applications. *Journal of Materials Science: Materials in Electronics*, 31(3), 2481–2496. https://doi.org/10.1007/s10854-019-02785-w
- Li, J., Wang, W., Liu, B., Duan, G., & Liu, Z. (2020). Enhanced Dy3+ white emission via energy transfer in spherical (Lu,Gd)3Al5Ol2 garnet phosphors. *Scientific Reports*, 10(1), 2285. https://doi.org/10.1038/s41598-020-59232-8
- Linganna, K., Haritha, P., Venkata Krishnaiah, K., Venkatramu, V., & Jayasankar, C. K. (2014). Optical and luminescence properties of Dy3+ ions in K–Sr–Al phosphate glasses for yellow laser applications. *Applied Physics B*, 117(1), 75–84. https://doi.org/10.1007/s00340-014-5801-6
- Mahamuda, Sk., Syed, F., Annapurna Devi, Ch. B., Swapna, K., Prasad, M. V. V. K. S., Venkateswarlu, M., & Rao, A. S. (2021). Spectral characterization of Dy3+ ions doped phosphate glasses for yellow laser applications. *Journal of Non-Crystalline Solids*, 555, 120538. https://doi.org/10.1016/j.jnoncrysol.2020.120538
- Mika, A., Sek, G., Ryczko, K., Kozub, M., Musial, A., Marynski, A., Misiewicz, J., Langer, F., Höfling, S., Appel, T., Kamp, M., & Forchel, A. (2013). Oscillator strength of optical transitions in InGaAsN/GaAsN/GaAs quantum wells. *Optica Applicata*, 43(1), 53–60. https://doi.org/10.5277/oa130107
- Milanese, D., P. D., B. N. G., C.-G. E., J. D., S. V. M., V.-B. C., & L. J. (2017). Phosphate glass fibers for optical amplifiers and biomedical applications. *Optical Fiber Communication Conference*, OFC 2017, (pp. M2F-2). OSA.
- Nath, P., & Biswas, A. (2023). Model development of lattice-matched p-GaInP/i-GaAs/n-GaInP hetero-junction solar cell and its performance optimization. *Optical Materials*, 143, 114155. https://doi.org/10.1016/j.optmat.2023.114155
- Neupane, C. P., Sylvester, J., Mudiyanselage, D. M. S. R., Singhapurage, H. A. S., & Ganikhanov, F. (2022). Ultrafast Phonon Decay in Complex Oxides. *Optics*, 3(4), 438–446. https://doi.org/10.3390/opt3040037
- Norkus, M., Skruodienė, M., Niaura, G., Šarakovskis, A., & Skaudžius, R. (2021). New low-temperature phosphate glasses as a host for Europium Ions. *Journal of Non-Crystalline Solids*, *569*, 120966. https://doi.org/10.1016/j.jnoncrysol.2021.120966
- Panggabean, J. H., Sihombing, L. W., Rajagukguk, J., Sarumaha, C. S., & Kaewkhao, J. (2024). Effect of Boric Oxide Compounds on the Physical Properties and Structure of "Huta Ginjang" Quartz Sand-Based Glass Medium. *Journal of Physics: Conference Series*, 2908(1), 012008. https://doi.org/10.1088/1742-6596/2908/1/012008
- Sharma, S., R. D. K., & R. S. B. (2018). Luminescence enhancement in fosfat glasses doped with Dy<sup>3+</sup> ions. *Optik International Journal for Light and Electron Optics*. Vol 22, (pp. 82-90).
- Shen, B., Zhang, Y., Zhang, Y., & Hu, J. (2020). Investigation of upconversion luminescence for Tb3+/Yb3+ codoped CaLnAlO4 (Ln = Y, Gd, La) phosphors. *Journal of Luminescence*, 223, 117266. https://doi.org/10.1016/j.jlumin.2020.117266
- Thakur, S. N. (2020). Atomic emission spectroscopy. In *Laser-Induced Breakdown Spectroscopy* (pp. 23–40). Elsevier. https://doi.org/10.1016/B978-0-12-818829-3.00002-2
- Thanyaphirak, W., Yasaka, P., Boonin, K., Sangwaranatee, N., & Kaewkhao, J. (2024). DY<sup>3+</sup> Ion Doped Zinc Barium Niobium Boro-Tellurite Glasses: Structural, Optical, and Luminescence Insights for White Light Applications. *Suranaree Journal of Science and Technology*, 31(3), 030199(1-9). https://doi.org/10.55766/sujst-2024-03-e06013
- Ullah, I., Zaman, F., Rooh, G., Khattak, S. A., Khan, I., Shoaib, M., Kaewkhao, J., Wabaidur, S. M., & Islam, M. A. (2022). Photoluminescence and energy transfer investigations in Gd3+-Dy3+co-doped borate glasses. *Physica B: Condensed Matter*, 639, 413976. https://doi.org/10.1016/j.physb.2022.413976
- Zhuk, N. A., Sekushin, N. A., Sivkov, D. V., & Popov, A. V. (2023). Electrical properties of Co-doped CaCu3Ti4O12. *Ceramics International*, 49(2), 2486–2494. <a href="https://doi.org/10.1016/j.ceramint.2022.09.223">https://doi.org/10.1016/j.ceramint.2022.09.223</a>
- Zekri, M., Herrmann, A., Turki, R., Rüssel, C., Maâlej, R., & Damak, K. (2019). Experimental and theoretical studies of Dy3+ doped alkaline earth aluminosilicate glasses. *Journal of Luminescence*, 212, 354-360.